atmosphere

Article

A Comparative Analysis between Radar and Human Observations of the Giant Hail Event of 30 August 2022 in Catalonia

Tomeu Rigo *,† and Carme Farnell †

Servei Meteorològic de Catalunya, Dr. Roux, 80, 08017 Barcelona, Spain; carme.farnell@gencat.cat
* Correspondence: tomeu.rigo@gencat.cat
† These authors contributed equally to this work.

Abstract: Three facts characterise the hailstorm of 30 August 2022 in the Catalan village of La Bisbal d'Empordà and its surroundings: first, the most dramatic, the death of a child hit by a hailstone; second, the damage to most of the roofs and cars in the town; finally, the highest recorded amount of hail (more than 10 cm) in Catalonia in at least the last 30 years. This research focuses on the radar field comparison and the observations provided by an electronic survey of the study area. The results reveal that weather radar underestimated the hail size because of different factors. Conversely, some reporters provided an inaccurate hour. The difference of three months between the hail event and the electronic survey is the probable cause of this mistake in the time estimation. However, the survey delay helped to avoid answers with larger hail sizes than those provided by the official spotters.

Keywords: giant hail; field work; hailstorm; damages; weather radar

check for updates

Citation: Rigo, T.; Farnell, C. A Comparative Analysis between Radar and Human Observations of the Giant Hail Event of 30 August 2022 in Catalonia. *Atmosphere* **2023**, *14*, 1190. https://doi.org/10.3390/atmos14071190

Academic Editor: Matthew Eastin

Received: 24 May 2023
Revised: 19 June 2023
Accepted: 22 July 2023
Published: 24 July 2023

1. Introduction

Allen et al. [1] summarised the state-of-art of the different fields regarding hail events (from the favourable environmental conditions to the internal structure of hailstones) in a deep review of the literature. The main points were a global increase in the costs caused by hailstorms [2], the improvement (though not enough) of the remote sensing techniques for diagnosing hail [3–5], and the influence of global warming in the increase in the severity of hail events. In this global context, but at a local scale, the afternoon of 30 August 2022 will remain in the memory of the inhabitants of La Bisbal de l'Empordà (green pins labelled as "S1" and "S2" in Figure 1) and the surrounding villages for decades. The small town was hit by the most destructive hailstorm that occurred in the Iberian Peninsula in the last few years. Large hailstones of 10 cm in diameter fell in a city of 11,000 inhabitants and produced much damage to the population (1 little girl died and more than 60 people were injured) and to the infrastructure (most cars and roofs suffered impacts with economic losses over EUR 5.6 million [6]). The event had repercussions in the meteorological community around the world (see, for instance, the report of the European Severe Storm Laboratory [7]).

Cases of hailstorms in Catalonia are frequent and have led to different analyses of the associated atmospheric patterns [8], campaigns for developing tools to diagnose hail in thunderstorms [9], and the implementation of nets for protecting crops in identified regions [10]. Furthermore, Farnell et al. [11,12] studied the thermodynamics associated with the different types of precipitation, from liquid to large hail. However, the affected area and the hail size are the first questions of interest; the region is usual for these types of storms, but, on the other hand, the size is much larger than the historical records, based on analyses such as [13,14].

Figure 1. Area hit by the hailstorm on 30 August 2022. The green pins indicate the locations of the three points of the field work, the orange points show the positions with information provided thorough the electronic form, and the solid lines delimit the areas of Vertical Integrated Liquid (VIL) from radar of 15 mm (orange), 35 mm (red), and 55 mm (purple). The top-right panel marks the area (white rectangle) in a map of Europe.

The combination of radar fields with ground registers [15,16] has allowed confirmation of the high spatial variability in the amount of hail that falls in the region of study, in a similar way to other countries around the world [1,17–19]. In this way, field work becomes a crucial tool for understanding the hailfall nature, allowing deeper dives into the improvement of diagnosis and forecasting tools [20]. One operational use of the weather radar in Catalonia in recent years has been the delimitation of the area of affectation by hailfall through the VIL product (see Figure 1 and [21]).

Regarding the hail size, the largest registered size in Catalonia was 7 cm until the event of analysis, according to the literature [16]. However, giant hail (that is, stones with diameter over 10 cm [4]) is not uncommon in the United States [22,23], Argentina [24], or, more recently, in the Mediterranean [25,26]. The objective of this work is to present the comparison results between some radar fields and a survey completed some months later than the event occurrence. The research was carried out by combining direct analysis with the information provided by different sources, through an electronic survey, and from the visual reports and other data given by some spotters. The final goal is to contextualise the event regarding the spatial variability and the extraordinariness with regard to other cases in Catalonia, the Mediterranean Basin, and around the world.

2. Materials and Methods

2.1. Study Area

Figure 1 shows the area of study, which is the northeastern part of Catalonia (located in the NE of the Iberian Peninsula). The region is known as the Empordà, marked with a white rectangle in the top-right panel of the figure, and the total extent considered has an area of 12,416 km^2 (including a part of the sea and some neighbouring counties). The hailstorm of 30 August 2022 hit a large part of the area inside the solid orange line region.

The event epicentre was La Bisbal d'Empordà and its surroundings. It is the capital of the Southern Empordà county and has a population of 11,000 inhabitants. Figure 2 shows the limits of the village (in red) and of Corçà, a tiny town to the NW of the first location (the limits marked in blue). This region has an area of 20 km^2. According to the Catalan Institute of Statistics (https://www.idescat.cat/indicadors/?id=aec&n=15227, accessed on 12 June 2023), the population density is 178 inhabitants per km^2. However, if we focus on the epicentre of the event, this value decreases to 90 inhabitants per km^2, ranging between 10 (inland area) and 450 (coastal municipalities) inhabitants per km^2, depending on the municipality. These values are far from the 2000 inhabitants per km^2 for the Catalan Central Coast of Catalonia. Furthermore, there are many municipalities with fewer than 2000 inhabitants. The sector of the population between 16 and 64 years old is 66% of the total, but, in the smallest villages, this value is biased toward the older sector.

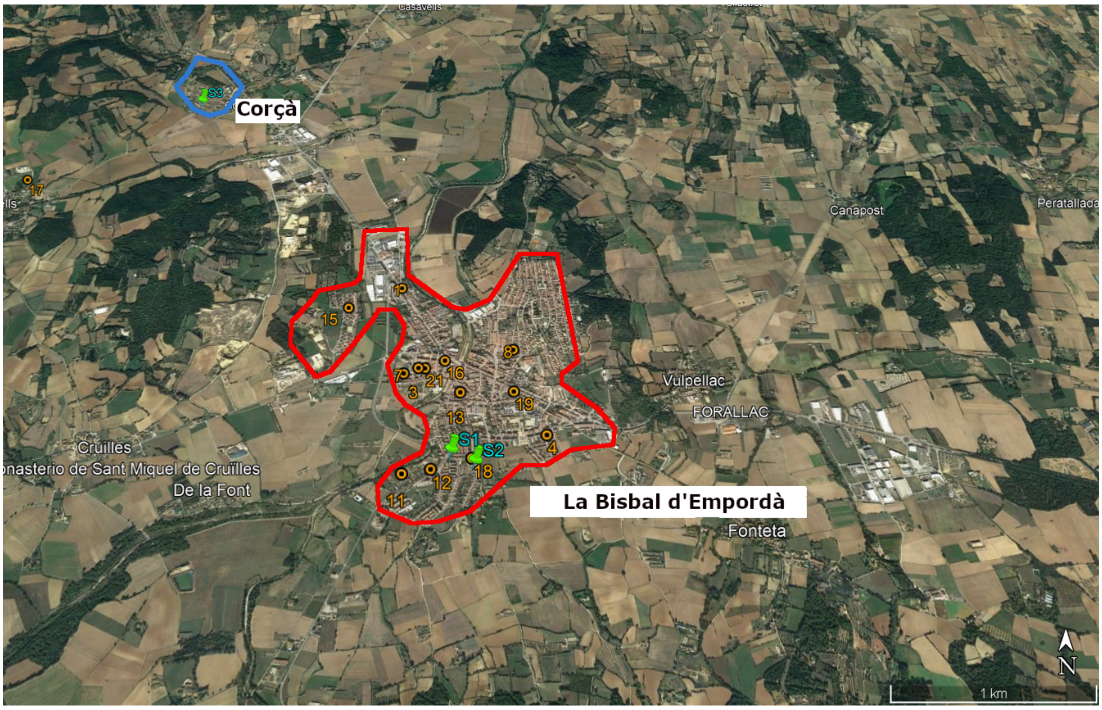

Figure 2. Zoomed-in image of La Bisbal d'Empordà (marked with a red line) and Corçà (delimited by a blue line). The green pins correspond to the locations of the field work and the orange points mark the positions with information provided in the form.

Figure 3 shows the hail swath generated using radar data, delimited by the purple line. The yellow line marks the transect considered for generating the vertical prole of the elevation (topography), presented in the bottom panel of the figure. It is possible to distinguish two differentiated terrains: in the first 25 km of the trajectory, including the onset of the thunderstorm, heights between 1360 and 250 m a.s.l. in steep terrain; and, from 25 to 85 km (where the thunderstorm reached the coastline), the land was mostly planar, with elevations between 250 and 0 ma.s.l., with progressive and soft downward slopes.

According to the Catalan Severe Weather Database (CSWD) of the Servei Meteorològic de Catalunya (SMC) [14], there have been 94 days with hail recorded in the study area since 2008. There was only one registered on 51 of these days. This fact indicates that most of the hail events were very local. On the contrary, only nine days registered more than four hail observations. Most of the 199 observations (67.8%) corresponded to small hail ($\leq$1 cm), while 24.1% were large hail ($\geq$2 cm). These values indicate that hail and large hail are usual in the area, but are less common than other parts of Catalonia [14].

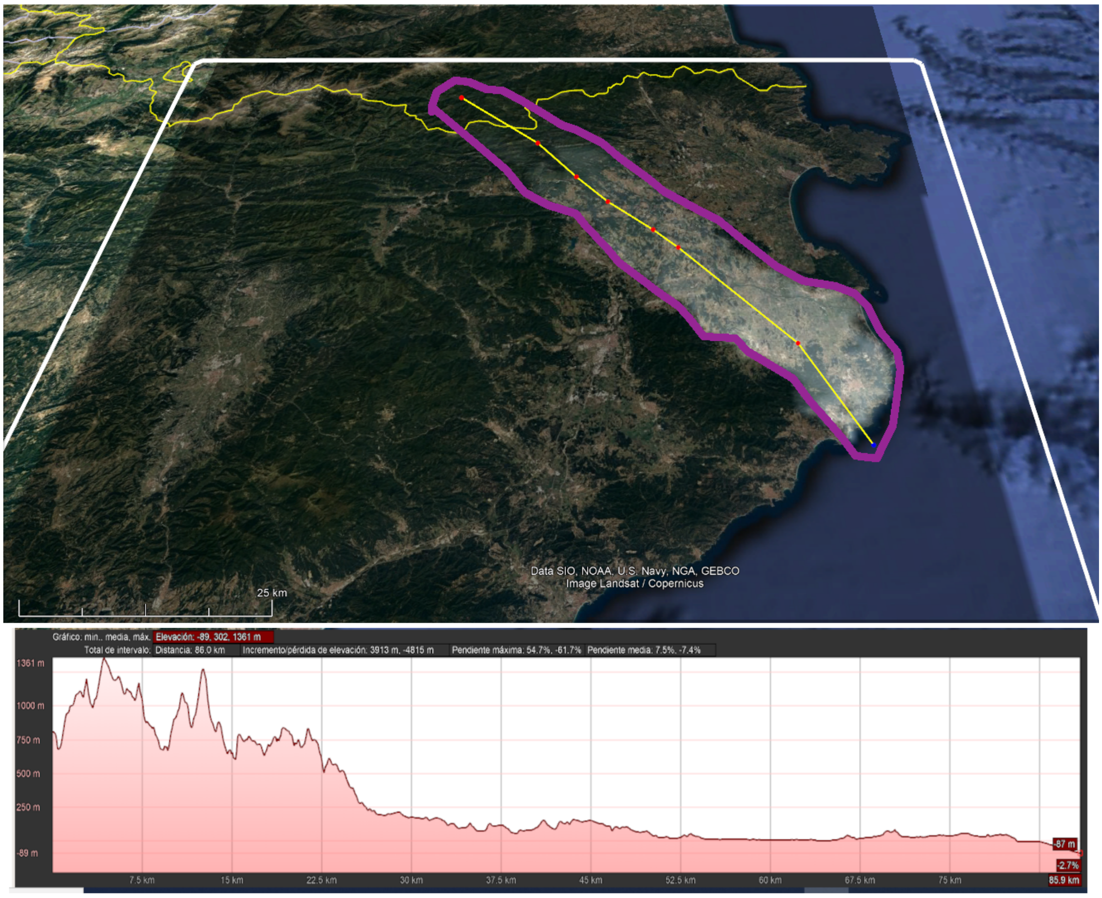

Figure 3. (**Above**) Track of the hailstorm delimited by the purple solid lines. The yellow line indicates the section of the vertical profile of the elevation. (**Below**) Vertical profile of the elevation.

2.2. Data Used

2.2.1. Radar Data

We used the maximum daily VIL product of the composite of the Radar Network (hereafter, XRAD) of the Servei Meteorològic de Catalunya for delimiting the region of interest. The XRAD consists of four C-Band single-pol radars covering the whole territory of Catalonia at different vertical levels (depending on the distance to the radars and the beam blockage of each part of the region). Each radar generates a full volume with a time resolution of 6 min—the same resolution as all the different products, including the composite VIL. The operative spatial resolution is 1 km $\times$ 1 km and uses the maximum value of the 4 radars at each field pixel. However, we used an experimental spatial resolution of 150 m $\times$ 150 m. The maximum daily field is generated at the end of the day using the 240 composite maps. The affected area estimation was similar to that in [21]. In that previous study, the selected optimal VIL threshold was 20 mm, according to the ground reports of affectation in crops.

2.2.2. Form Results

After different conversations with some spotters in the regions, the technicians of the Servei Meteorològic de Catalunya created an online survey which was spread through social networks. The posed questions were as follows:

(1) What are the coordinates of your location?;
(2) At what time do you think the event occurred at your location?;
(3) What was the duration of the event?;
(4) What was the maximum size of the stones?;
(5) Were all the stones regular in size?

It is worth noting that we delivered the form three months after the event. This delay served two purposes. The first was to reduce the exaggeration of the observations, following the literature [27–30]. One of the main limitations of the survey is the format itself. Performing an online survey, we were aware that most small villages (with old and small populations, as was presented before) would have a null or residual representation. In any case, the main towns had at least one answer. However, these answers had great value, because they were supposed to be accompanied by a picture of the hailstones. Of course, it was impossible to remove the bias caused by the population density (see the Study Area section for more details) in this research because we searched for registers at the exact time of the event. We were not interested in those observations provided some hours after, when people moved to farms or small villages to observe the damages in their properties. Furthermore, by making a matrix with 4 km $\times$ 4 km grid resolution for the analysis area, we found that 10 of the 42 pixels had at least 1 register. This grid resolution corresponded to that suggested by Farnell and Rigo [16] in a comparison between ground observations and radar fields. The second purpose was to minimise the effect on the observers caused by the damage claims to insurance and other administrations. The values were more biased in agricultural areas, as was found in other presented analyses [31,32]. Changnon observed that the bias in hail size estimation was at less 0.1 cm in stones greater or larger than 2.5 cm. A complementary point is the difficulty in comparing remote sensing data and ground observations, as some research has shown before [16,33,34].

3. Results

3.1. Description of the Event: A Comparison between Radar Data and the Electronic Form

The electronic form contained 28 valid answers that provide valuable information about the event. Twenty of the reports corresponded to La Bisbal de l'Empordà, allowing a very detailed composition of the event for the city (reports covered practically all the districts). We compared this information to the VIL composite product (for 6-minute periods and the maximum daily field). The rest of the reports, more dispersed, also helped to validate the radar product performance in areas far from the epicentre that also showed some damages. This section describes the event from the point of view of the testimonies, according to their comments to the different suggested questions.

3.1.1. Time of Occurrence of the Event

The first question asked was as to what time the hailfall occurred. Not all the registers corresponded to the indicated coordinates. If we mark La Bisbal d'Empordà as the epicentre of the event, we can define, as the origin, the coordinates of the city centre: 41.959012° N, 3.037783° E. The highest points and lowest latitudes were 17 km north and 5 km south, respectively, while the extreme longitude registers were 5 km west and 10 km east. All the observations were integrated into the box (as shown in Figure 4).

Figure 5 shows the pie charts of the time of occurrence of the hailfall, according to the different answers to the survey. The left panel shows the results for all the collected cases, while the right focuses exclusively on the registers in the epicentre. According to the radar imagery, the thunderstorm hit the area shown in the right panel of Figure 4 between 17.00 and 18.00 UTC (19.00 and 20.00 local time), and La Bisbal between 17.30 and 17.40 UTC (19.30 and 19.40 LT). One of the interesting points is that many observers in La Bisbal provided the wrong time: only seven of the fourteen registers agreed with the radar observations. The difference in time between the event and the answers to the form could have been caused by the discrepancy between radar and ground. In any case, the lag time is the most difficult to answer, because it needs an awareness of time that is difficult to apply in events in real time. Furthermore, the observer was asked to provide the answer in this case without any help, while, on the contrary, they could choose between different possible responses for the rest of the questions.

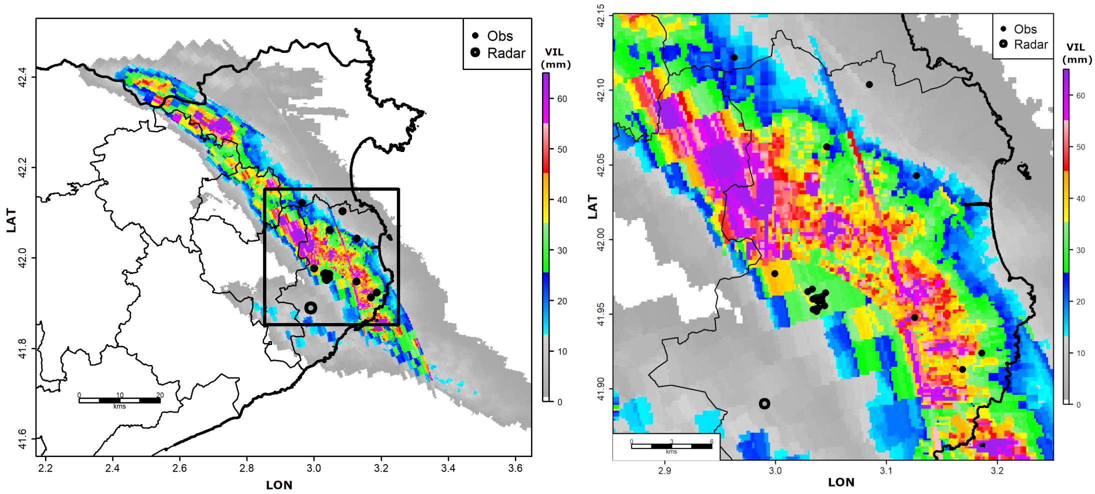

Figure 4. (**Left**) Maximum daily VIL field (in mm) of the event. The black dots correspond to the registers and the largest black and grey dots indicate the location of the closest radar. (**Below**) Zoomed-in image of the region with registers, corresponding to the black square in the left panel.

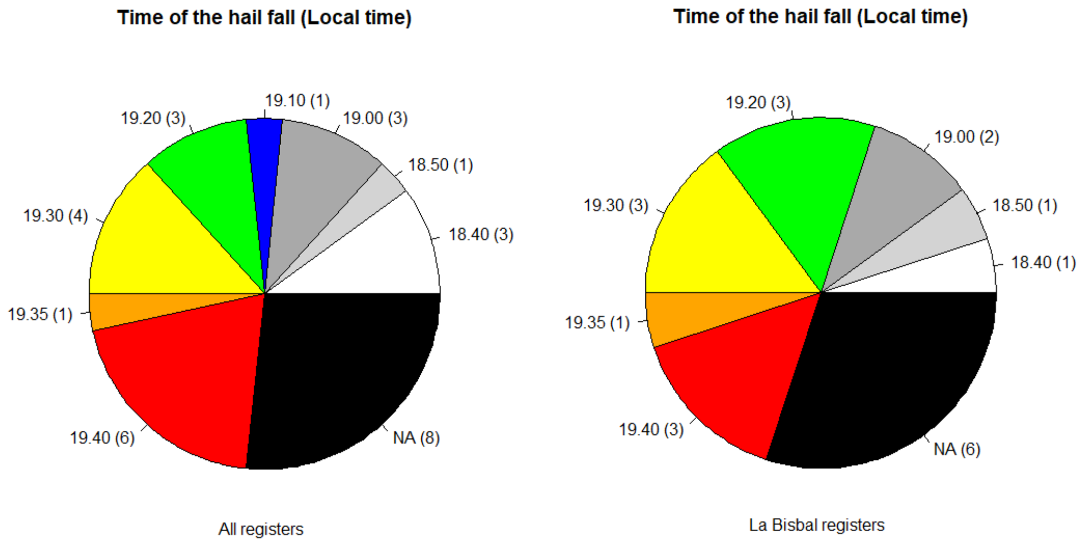

Figure 5. (**Left**) Pie chart with the time (local time, +2 h with respect to UTC) of all the registers. (**Right**) The same as the left panel, but only for the La Bisbal de l'Empordà cases.

3.1.2. Duration of the Event

The second item of interest in the survey was the duration of the hailfall (Figure 6). According to many testimonies gathered by television reporters on the same day of the event, the hailstones precipitated over La Bisbal for a very long time (some of the testimonies said, "It seemed that the hail did never stop to fall, and the size increased as the event evolved"). Accordingly, the possible options were "less than 2 min", "between 2 and 5 min", "between 5 and 10 min", and "more than 10 min".

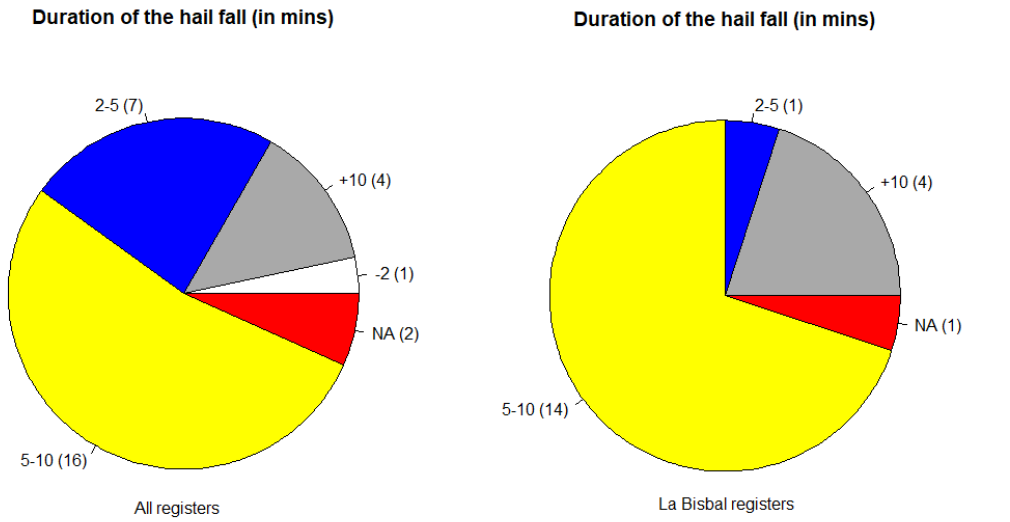

Figure 6. (**Left**) Pie chart with the duration of the event for all registers. (**Right**) The same but only for La Bisbal d'Empordà observations.

The event duration results showed interesting information. First, the case of reduced duration (less than 2 min) occurred far from the epicentre, as did most of the observations of short duration (between 2 and 5 min). Only one testimony of the epicentre area provided one of the seven answers of short duration. Then, the percentage of cases of the short duration category moved from 23.3% (all registers) to only 5% (La Bisbal). On the contrary, the percentage of answers in the category of long duration (between 5 and 10 min) increased from 53.3% for the whole area to 70% at the epicentre. Similar behaviour occurred with the very long duration category: all the cases were provided by La Bisbal testimonies, with a change from 13.3% to 20%.

The previous values agreed with the radar fields, which indicated that the thunderstorm core crossed La Bisbal in the mature stage. On the contrary, the central part of the storm partially hit other populations, or hit when it was in a less active phase. Searching for some comparable values in the literature, we only found the data provided by [35] for the SW of France, who indicated values between 2 and 45 min, with a mean duration of 11.5 min (but for stones of less than 2 cm in diameter), or by [36] for Switzerland, with 9 cases between 6 and 25 min in duration. Nevertheless, these results provide a first approach to the duration in the case of giant hail.

3.1.3. Maximum Size of the Stones and Homogeneity

We merged two questions (what was the maximum size of the stones? and "Were the stones of similar size?") into the same item: what was the behaviour of the hailfall? In addition to asking for some testimonies during the fieldwork, we realised that other points were also important. One of them was how the event evolved. In all the reports, the description was the same: the episode started with large hailstones falling separated by some time (some seconds) and space (about ten meters), passing to frequencies of less than one second and very close stones in the mid-part of the event. Additionally, the hailfall was mostly dry (without liquid rainfall), except at the end.

Moving to the maximum size, Figure 7 summarises the differences between all the regions, with a focus on the epicentre. In the second case, there were only answers over 4 cm, but 65% of the testimonies indicated that larger hailstones exceeded the diameter of 8 cm. On the contrary, 20% of the cases in the total area had maximum sizes below 4 cm (including La Bisbal values). Thus, we can affirm that there existed a homogeneity in the occurrence of giant hail in the event epicentre, but this disappeared as the storm progressed farther from La Bisbal. However, this point is different with regard to the question about the variability in the size of the stones at a location (are all of them of a similar size at that point during all the events?). Only two testimonies from La Bisbal and two others from the rest of the area answered positively to that question. Surprisingly, in the case of the epicentre, both observers reported sizes of more than 8 cm (i.e., they affirmed that hail was of that size during the event), while, in the other two cases, the maximum hail sizes reported were less than 1 and between 2 and 4 cm. In any case, most of the testimonies confirmed the heterogeneity of the stones' size, agreeing with previous analyses, such as [37].

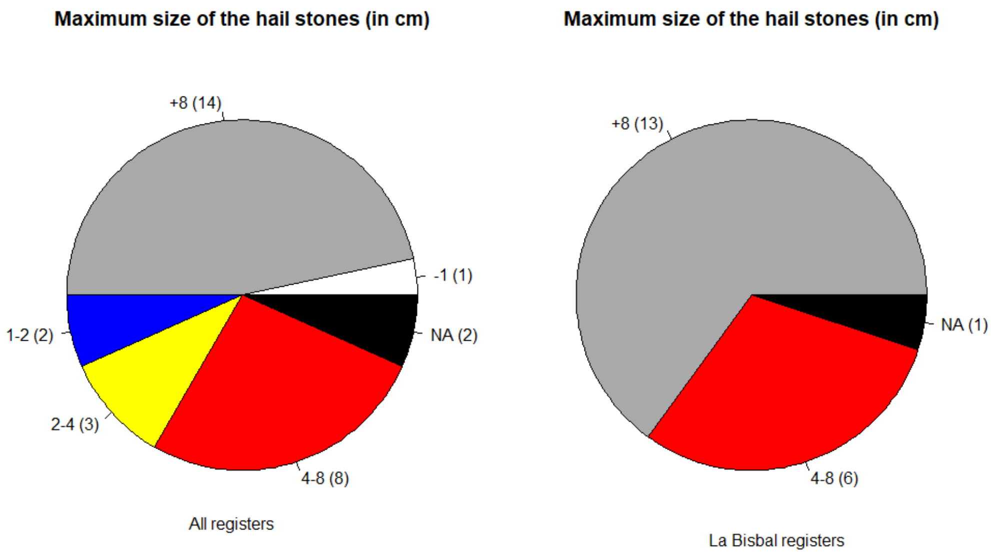

Figure 7. (**Left**) Pie chart with the maximum size of the stones for all surveys. (**Right**) The same, but only for La Bisbal d'Empordà observations.

3.2. Map of Maximum Size

Following the research performed in [16], we tried to estimate the field of the maximum size of the stones, combining the radar information and the ground survey responses. The combination technique consists of geo-statistical methods, in which the radar field provides the shape of the new map while the reports give quantitative information. As in previous research, universal co-Kriging was the selected interpolation technique.

In the previous analysis, the radar field that fitted best was the VIL. However, there was a lack of coherence in the product concerning the ground observations, as shown in Figure 4. The values in the epicentre (hail diameter larger than 8 cm) were lower than 40 mm, while, in other regions with lower values of hail size, the VIL exceeded 55 mm (Figure 8). The causes of these anomalies are as follows. First, the distance of most of the radars from the area of interest (more than 100 km except for PDA -Puig d'Arques- radar), making their contribution poor. Second, the thunderstorm moved quasi-perpendicularly to the PDA radar, affecting the higher levels when the cloud was too close to the radar (less than 20 km). These first two causes are associated with the same product configuration, which is highly dependent on the vertical profile of reflectivity at each point [3]. The third and final cause was the attenuation of the radar signal caused by the large hail, agreeing with the observations of [38].

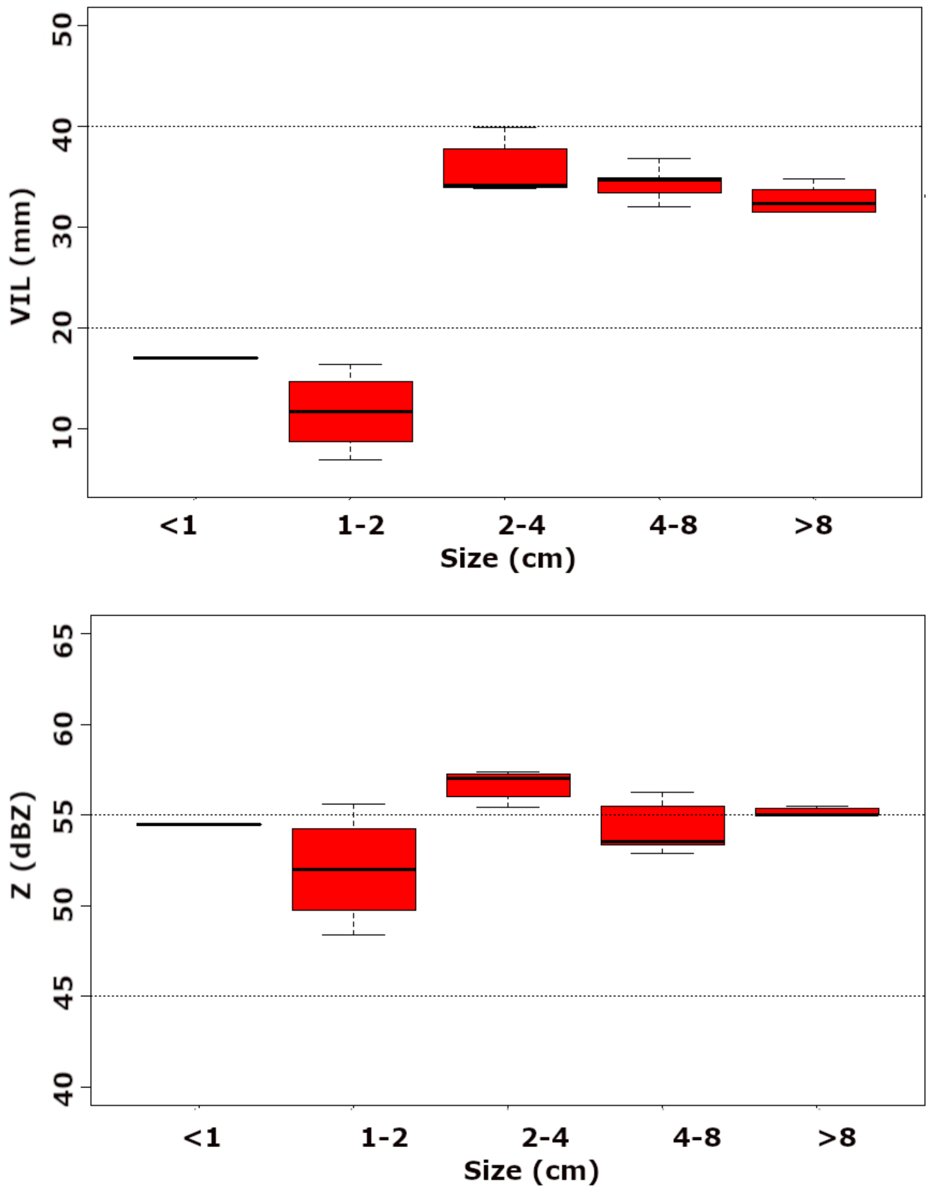

Figure 8. Boxplot of the different pixels with ground registers grouped by size for the VIL (**above**) and the maximum reflectivity (**below**) daily fields.

To minimise the previous limitations (and following the proposal of [16]), we selected the maximum reflectivity field as the radar predictor field. In this case, the daily maximum reflectivity map (Figure 9) and the boxplots (bottom panel of Figure 8) were more coherent with the ground registers. This coherence appeared in the epicentre of the event, where the values of the reflectivity were more in agreement with the ground observations than VIL, and with the evolution of the boxplot categories—the larger reported hailstones (8 cm) presented at least similar values compared to other categories (2–4 cm or 4–8 cm).

Figure 10 presents the results of applying the Universal co-Kriging technique. The top panels (a and b) show the results for the event epicentre, using, as predictors, the VIL and the maximum reflectivity, respectively. The first radar product cannot reproduce the nature of the hailfall, reducing the area of giant hail (A5) to the event epicentre (La Bisbal). On the contrary, the area with large hailstones over 8 cm, estimated using maximum reflectivity, seems over-sized, according to the ground observations. Similar behaviour occurs for the total hit area (panels c and d), with an underestimation for the VIL product and an overestimation for maximum reflectivity. However, both fields allow an understanding of the nature of the hail-swath and can help to identify areas of affectation with different landscapes (e.g., in pine forest [39]).

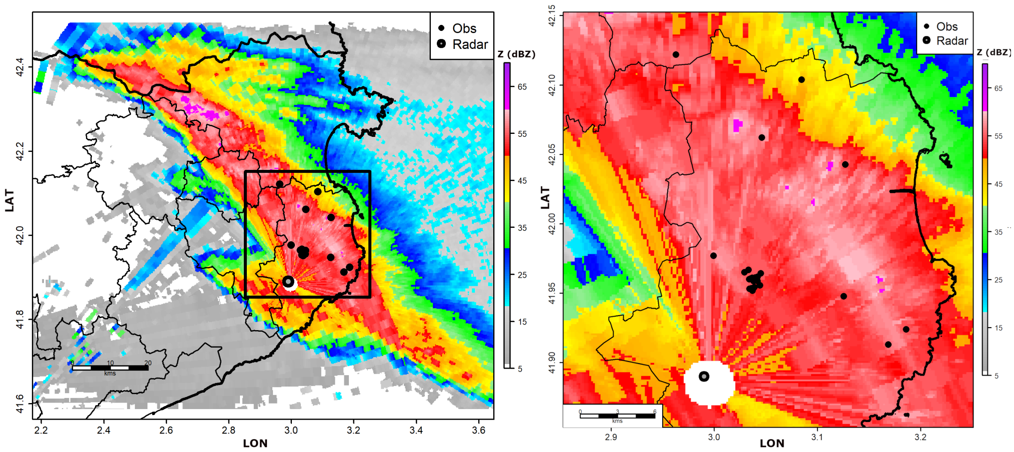

Figure 9. The same as Figure 4, only using the maximum reflectivity.

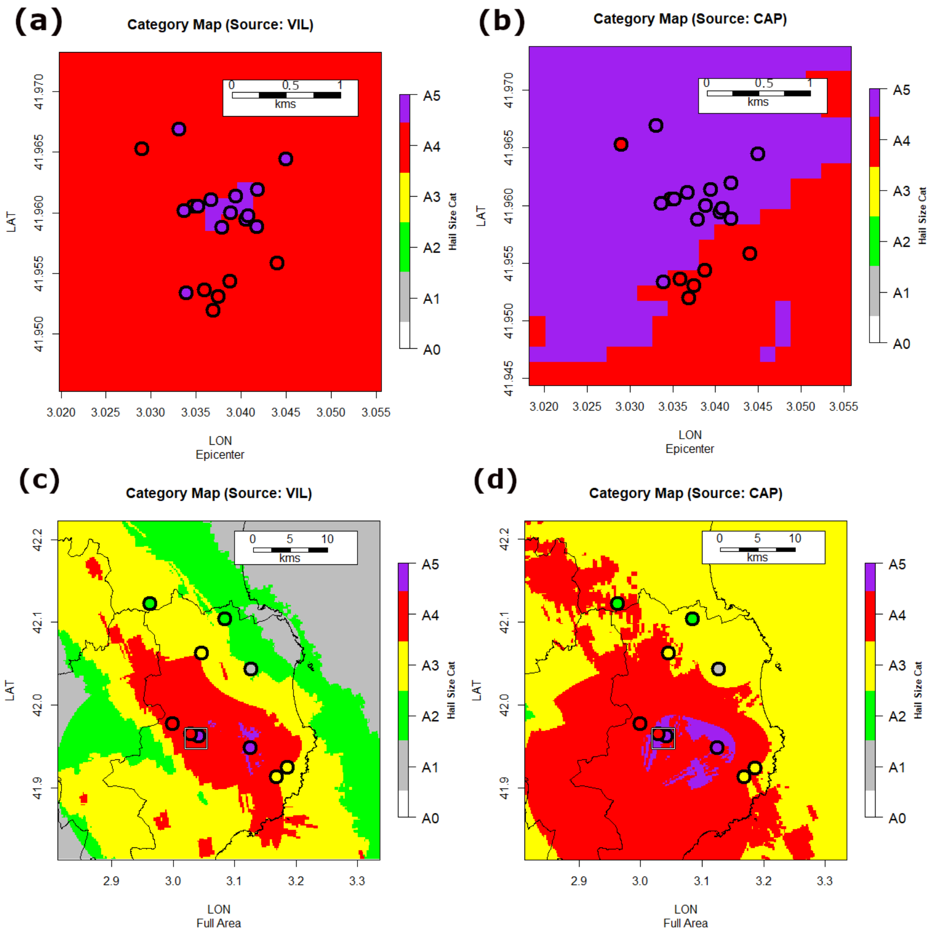

Figure 10. Maximum hail size field obtained from universal co-Krigging: (**a**) Using VIL for the epicenter; (**b**) Using maximum reflectivity for the epicenter; (**c**) as (**a**) but for the full area; (**d**) as (**b**) but for the full area. A0 indicates "No hail", A1: "hail $\leq$1 cm", A2: "hail 1–2 cm", A3: "hail 2–4 cm", A4: "hail 4–8 cm", and A5: "hail $\geq$8 cm".

3.3. Comparison between Observations and Radar Fields

The last part of the research compared the information provided by the two sources: direct observations from the electronic survey, and the VIL radar field, over the locations of the ground registers. We first studied the differences between the time provided by the observers and the ones when VIL was not null over the same point. In this case, the radar acted as the observation. Second, we compared the VIL values over the location and the maximum size observed at the ground. Here, the reports were considered as ground truth. Before introducing the analysis, it is worth considering the different issues that could affect the results:

- The survey was made three months later, affecting the memory capacity of the contributors, especially concerning the time of occurrence. However, this lag helped to minimise the effect of exaggeration of the hail size;
- VIL radar product was affected by different constraints presented previously: signal attenuation and distance of the hailstorm to the radars, among others.

Figure 11 shows three examples of the different behaviours observed concerning the time lag between the survey and the radar: (top) a case when the observation (cyan rectangle) in the survey was earlier than the real-time occurrence (based on the radar information); (centre) an example where the survey register and the radar field were simultaneous; (below) the time observer was delayed with respect to the radar data. These differences were mainly due to the time between the event and the survey. The VIL percentiles (25 in blue, 50 in yellow, 75 in orange, 90 in red, and max in purple) were estimated from all the pixels surrounding the coordinates provided by the observer within a radius of 2.5 km. The right column presents the location of the survey observations for each case (cyan point in the centre of each map). The top and bottom panels correspond to observations close in space, but one provided an advance time (by 30 min), while the other gave a delayed time (also by 30 min).

Tables 1 and 2 summarise the two points of interest. The first shows the difference between the survey estimation of the time of occurrence and the radar data. We considered the three options: advanced, synchronised, and delayed. Of these, 12 of the 20 valid observations (60%) were synchronised, indicating that most observers remembered the event evolution. From the out-of-time registers, most of them were ahead of time (6, i.e., 30% of the total), with a mean difference of 33 min. Oppositely, only 2 (10%) cases were delayed, with a mean difference of 10 min (clearly lower than the advanced cases). This behaviour had similitude to the one for the epicentre region, but the time error was larger than the global value.

Table 1. Number of cases of each behavior time of observation (survey) with respect to the real-time value (weather radar). The numbers in the parentheses indicate the cases in the epicentre.

	Advanced	**Synchronised**	**Delayed**
N cases	6 (4)	12 (8)	2 (2)

Concerning the capability of good size estimation through the VIL evolution, the previous section showed the limitations of the radar product. In the same way, Table 2 confirms the same performance for the individual observations. The underestimation was clear for all the cases except one in the epicentre (13 of 14, which is 65% of the total). On the contrary, the behaviour was quite good (three correct performances and three overestimating) for the rest of the regions, where the observations were lower (from less than 1 cm to between 4 and 8 cm). This fact confirms that the C-Band has high limitations in the cases of giant (and even large) hail because of the beam signal attenuation. Moreover, the proximity of the radar was not enough to minimise limitations.

Table 2. Number of cases of each behavior size of observation (weather radar) with respect to the real size (survey). The numbers in the parentheses indicate the cases in the epicenter.

	Underestimated	Right	Overestimated
N cases	13 (13)	4 (1)	3 (0)

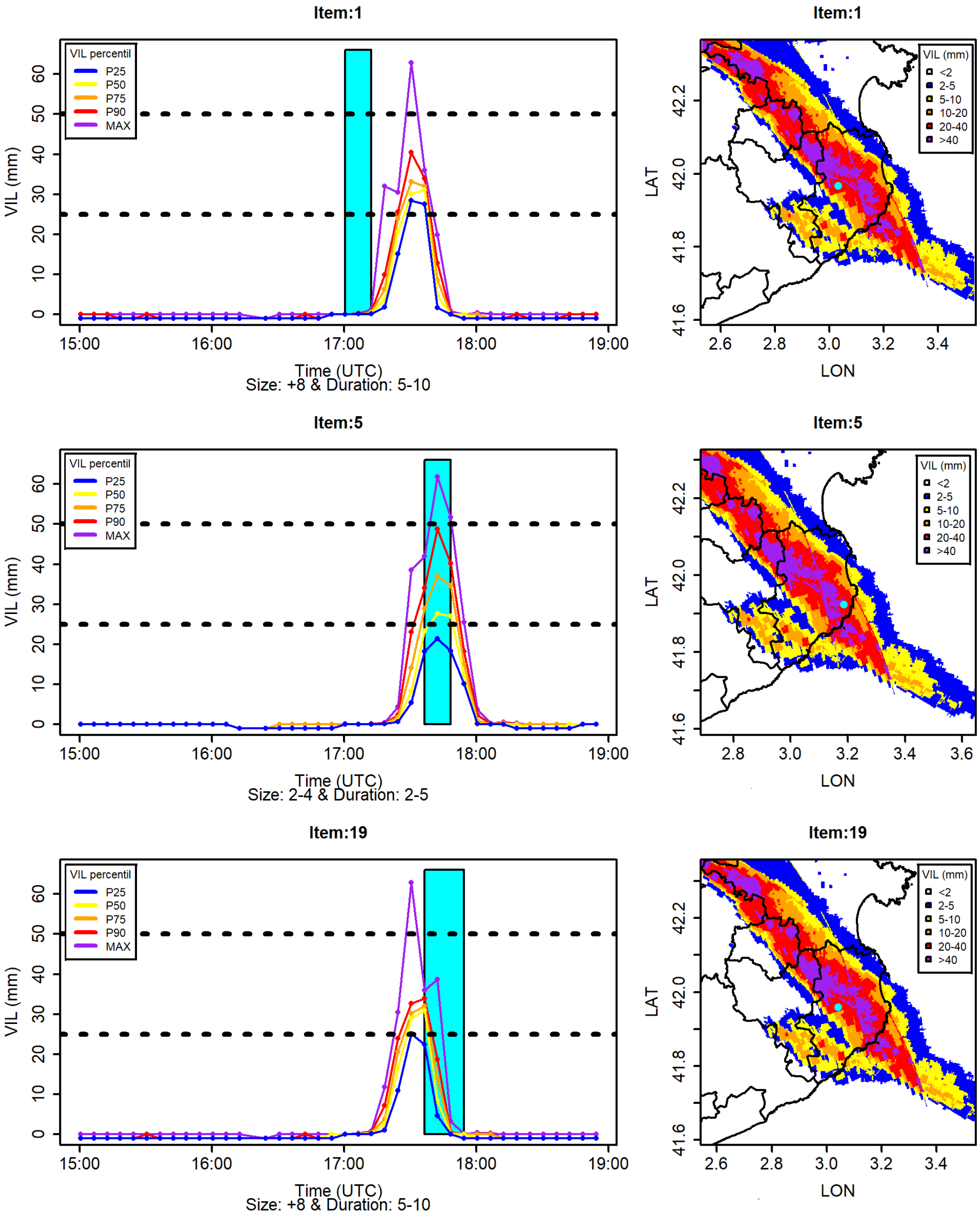

Figure 11. Different behaviors between VIL and the electronic survey. Left column: VIL evolution of the percentiles 25, 50, 75, 90, and the maximum over the location (cyan point on the right column maps). The cyan rectangles indicate the hail time (provided by the survey). The size and the duration are shown below the X-axis label "Time (UTC)". Right column: Maps showing the maximum daily VIL field in the surroundings of each observation. (**Top**) The survey indicated that the event occurred before the real time. (**Middle**) A case of simultaneity. (**Below**) A case of delay in the observation.

4. Discussion

This research has focused on comparing two different data sources to determine their ability to explain some characteristics of the giant hail event of 30 August 2022 in La Bisbal d'Empordà (NE of Catalonia). The data sources, on the one hand, are the results of an electronic survey. On the other hand, they were the maximum daily reflectivity and VIL composite radar parameters, with a spatial resolution of 150 m $\times$ 150 m and a time resolution of 6 min. We made the e-survey three months after the event to avoid hail size exaggeration, which is one of the issues from direct visual estimations [40]. The questions included in the survey were the following:

- Can you provide the exact location where you lived during the event?;
- What was the time of occurrence of the event?;
- How much time did it last?;
- What was the maximum size observed?;
- Were all the stones similar in size?

The results of the survey seemed of high quality, except for the point of the time of occurrence. The comparison with the evolution of the radar fields showed how some observers provided an advanced time ($\sim$35 min on average), while others gave delayed times ($\sim$10 min on average). Oppositely, sizes were quite consistent with the evolution of the episode and the data provided by the official spotters of the SMC.

According to many authors such as Ortega [34], Farnell [16], Changnon [32], and Saltikoff [33], the main issues of ground-based hail registers are as follows:

- The insufficient amount of data: In the present case, there are some areas with an evident lack of information, due to the low density population in the rural areas and the forest regions. However, the combination with the radar fields makes it possible to obtain an adequate estimation of the hail size in practically all the regions of interest. In any case, we preferred to avoid including data not validated correctly, especially those values without a picture, or those with a photograph that could not provide a comparison of the true size, because there was not an object of reference (a coin or a ruler);
- The biases provided by the economical interests: As was indicated before, we decided to wait a certain time before starting the form. The reason was that the high economical impact, caused mainly by damages in most of roofs in the epicenter of the region (La Bisbal and surroundings, as it was stated in the resolution of the Govern of the Generalitat of Catalonia—see https://residus.gencat.cat/web/.content/home/consultes_i_tramits_-_nou/subvencions/subvencions_mixtes/ajuts_amiant_meteo/resol_atorg_ACC_3194_2022_es.pdf —accessed on 14 December 2022), and the implications with regards to insurance and other economical assistance for many affected people. At the time of the initiation of the form, the economical assistance had arrived to most of those affected and they did not have a reason to exaggerate the size. In fact, some of the participants recognised that, after the three months period, they realised that the size was 1 or 2 cm less than their first estimations;
- The hail size accuracy reported: This point has a certain relationship with the previous one, but other reasons that exist other than economical reasons. People tend to provide exaggerated values of hail size, which are a consequence of the direct eye estimation without an adequate instrument to measure the diameter. For instance, some reporters provided observations of hailstones that were accurately measured after the form, because the reporters kept them in a freezer in optimal conditions. The result was differences of between 0.5 and 2 cm. The reporters confirmed that stones did not diminish in size because the stones were allocated in the same place where they were picked up.

To summarise, the delay of the form minimised the previous issues observed in most previous research. Furthermore, the radar fields (VIL and maximum reflectivity) allowed us to determine the temporal evolution of the event over each location. However, remote sensing fields suffered limitations in the size estimation, as was expected based on works such as [21,24,25]. The fact that the sizes were more than 8 cm in a lot of places and the proximity to one of the C-band single-pol radars (which cannot contribute to a part of the event because the radar volume was limited) agree with previous research [3,4,38]. Because of these limitations, it was impossible to reproduce an estimated field by combining both sources through geo-statistical analysis (Universal Co-Kriging) in a similar way that was used in Catalonia for previous events [16].

5. Conclusions

To sum up, the main conclusions of the analysis have been the following::

- The combination of observational data provided using an e-survey and some radar fields allowed a better understanding of different elements of the evolution of a giant hail event;
- The observations at the ground gave a better estimation of the size;
- The weather radar helped to have a better understanding of the evolution'
- It was not possible, however, to generate a maximum hail size field by combining both data because of the limitations of the weather radar in this type of giant hail size.

Author Contributions: Conceptualisation, T.R. and C.F.; methodology, T.R. and C.F.; software, T.R.; validation, C.F.; formal analysis, T.R.; investigation, T.R. and C.F.; resources, T.R. and C.F.; data curation, T.R.; writing—original draft preparation, T.R.; writing—review and editing, T.R. and C.F.; visualisation, T.R.; supervision, C.F. All authors have read and agreed to the published version of the manuscript.

Funding: This research received no external funding.

Institutional Review Board Statement: Not applicable.

Informed Consent Statement: Not applicable.

Data Availability Statement: Data are available upon e-mail request.

Acknowledgments: The Authors want to thank all the people of La Bisbal d'Empordà and the surroundings towns who contributed to the research with their testimony and, in some cases, with frozen hail. In particular, we want to thank Angel Galan for managing the preliminary process.

Conflicts of Interest: The authors declare no conflict of interest.

Abbreviations

The following abbreviations are used in this manuscript:

VIL	Vertical Integrated Liquid
XRAD	Radar Network of the Servei Meteorològic de Catalunya
UTC	Coordinated Universal Time
LT	Local Time
PDA	Puig d'Arques Radar

References

1. Allen, J.T.; Giammanco, I.M.; Kumjian, M.R.; Jurgen Punge, H.; Zhang, Q.; Groenemeijer, P.; Kunz, M.; Ortega, K. Understanding hail in the earth system. *Rev. Geophys.* **2020**, *58*, e2019RG000665. [CrossRef]
2. Brown, T.M.; Pogorzelski, W.H.; Giammanco, I.M. Evaluating hail damage using property insurance claims data. *Weather. Clim. Soc.* **2015**, *7*, 197–210. [CrossRef]
3. Boudevillain, B.; Andrieu, H. Assessment of vertically integrated liquid (VIL) water content radar measurement. *J. Atmos. Ocean. Technol.* **2003**, *20*, 807–819. [CrossRef]
4. Blair, S.F.; Deroche, D.R.; Boustead, J.M.; Leighton, J.W.; Barjenbruch, B.L.; Gargan, W.P. A radar-based assessment of the detectability of giant hail. *E-J. Sev. Storms Meteorol.* **2011**, *6*, 1–30. [CrossRef]
5. Punge, H.; Bedka, K.; Kunz, M.; Reinbold, A. Hail frequency estimation across Europe based on a combination of overshooting top detections and the ERA-INTERIM reanalysis. *Atmos. Res.* **2017**, *198*, 34–43. [CrossRef]

6. Rigo, T.; Rius, A. *Inform about the Estimation of the Hit Area by the Hailstorm of the 30 August 2022*; Technical Report of the Servei Meteorològic de Catalunya; Departament d'Acció Climàtica, Alimentació i Agenda Rural of the Generalitat de Catalunya, 18 September 2022. Available online: https://residus.gencat.cat/web/.content/aux_/comunes/docs/informe_area_afectacio_pedra_20220830.pdf (accessed on 14 December 2022). (In Catalan)
7. Pucik, T. On the Predictability of the Giant Hail Event in Catalonia. 2022. Available online: https://www.essl.org/cms/on-the-predictability-of-the-giant-hail-event-in-catalonia/ (accessed on 14 December 2022).
8. Aran, M.; Pena, J.; Torà, M. Atmospheric circulation patterns associated with hail events in Lleida (Catalonia). *Atmos. Res.* **2011**, *100*, 428–438. [CrossRef]
9. Aran, M.; Sairouni, A.; Bech, J.; Toda, J.; Rigo, T.; Cunillera, J.; Moré, J. Pilot project for intensive surveillance of hail events in Terres de Ponent (Lleida). *Atmos. Res.* **2007**, *83*, 315–335. [CrossRef]
10. Girona, J.; Behboudian, M.; Mata, M.; Del Campo, J.; Marsal, J. Effect of hail nets on the microclimate, irrigation requirements, tree growth, and fruit yield of peach orchards in Catalonia (Spain). *J. Hortic. Sci. Biotechnol.* **2012**, *87*, 545–550. [CrossRef]
11. Farnell, C.; Llasat, M.d.C. Proposal of three thermodynamic variables to discriminate between storms associated with hail and storms with intense rainfall in Catalonia. *Tethys* **2013**, *10*, 25–34. [CrossRef]
12. Farnell, C.; Rigo, T.; Heymsfield, A. Shape of hail and its thermodynamic characteristics related to records in Catalonia. *Atmos. Res.* **2022**, *271*, 106098. [CrossRef]
13. Rigo, T.; Farnell Barqué, C. Evaluation of the Radar Echo Tops in Catalonia: Relationship with Severe Weather. *Remote Sens.* **2022**, *14*, 6265. [CrossRef]
14. Farnell, C.; Rigo, T. The Lightning Jump, the 2018 "Picking up Hailstones" Campaign and a Climatological Analysis for Catalonia for the 2006–2018 Period. *Tethys* **2020**, *17*, 10–20. [CrossRef]
15. Farnell, C.; Rigo, T.; Pineda, N.; Aran, M.; Busto, M.; Mateo, J. The different impact of a severe hailstorm over nearby points. In Proceedings of the European Conference on Severe Storms, Helsinki, Finland, 3–7 June 2013; pp. 3–7.
16. Farnell, C.; Rigo, T.; Martin-Vide, J. Application of cokriging techniques for the estimation of hail size. *Theor. Appl. Climatol.* **2018**, *131*, 133–151. [CrossRef]
17. Hermida, L.; Sánchez, J.L.; López, L.; Berthet, C.; Dessens, J.; García-Ortega, E.; Merino, A. Climatic trends in hail precipitation in France: Spatial, altitudinal, and temporal variability. *Sci. World J.* **2013**, *2013*, 494971. [CrossRef] [PubMed]
18. Marcos, J.; Sánchez, J.; Merino, A.; Melcón, P.; Mérida, G.; García-Ortega, E. Spatial and temporal variability of hail falls and estimation of maximum diameter from meteorological variables. *Atmos. Res.* **2021**, *247*, 105142. [CrossRef]
19. Dalezios, N.R.; Loukas, A.; Bampzelis, D. Universal kriging of hail impact energy in Greece. *Phys. Chem. Earth Parts A/B/C* **2002**, *27*, 1039–1043. [CrossRef]
20. Farnell, C.; Busto, M.; Aran, M.; Andrés, A.; Pineda, N.; Torà, M. Study of the hailstorm of 17 September 2007 at the Pla d'Urgell. Part one: Fieldwork and analysis of the hailpads. *Tethys* **2009**, *6*, 69–81.
21. Rigo, T.; Farnell, C. Using maximum Vertical Integrated Liquid (VIL) maps for identifying hail-affected areas: An operative application for agricultural purposes. *J. Mediterr. Meteorol. Clim.* **2019**, *16*, 15–24. [CrossRef]
22. Witt, A.; Burgess, D.W.; Seimon, A.; Allen, J.T.; Snyder, J.C.; Bluestein, H.B. Rapid-scan radar observations of an Oklahoma tornadic hailstorm producing giant hail. *Weather. Forecast.* **2018**, *33*, 1263–1282. [CrossRef]
23. Gutierrez, R.E.; Kumjian, M.R. Environmental and radar characteristics of gargantuan hail–producing storms. *Mon. Weather. Rev.* **2021**, *149*, 2523–2538. [CrossRef]
24. Kumjian, M.R.; Gutierrez, R.; Soderholm, J.S.; Nesbitt, S.W.; Maldonado, P.; Luna, L.M.; Marquis, J.; Bowley, K.A.; Imaz, M.A.; Salio, P. Gargantuan hail in Argentina. *Bull. Am. Meteorol. Soc.* **2020**, *101*, E1241–E1258. [CrossRef]
25. Montopoli, M.; Picciotti, E.; Baldini, L.; Di Fabio, S.; Marzano, F.; Vulpiani, G. Gazing inside a giant-hail-bearing Mediterranean supercell by dual-polarization Doppler weather radar. *Atmos. Res.* **2021**, *264*, 105852. [CrossRef]
26. Papavasileiou, G.; Kotroni, V.; Lagouvardos, K.; Giannaros, T.M. Observational and numerical study of a giant hailstorm in Attica, Greece, on 4 October 2019. *Atmos. Res.* **2022**, *278*, 106341. [CrossRef]
27. Allen, J.T.; Tippett, M.K. The characteristics of United States hail reports: 1955–2014. *E-J. Sev. Storms Meteorol.* **2015**, *10*, 1–31. [CrossRef]
28. Cintineo, J.L.; Smith, T.M.; Lakshmanan, V.; Brooks, H.E.; Ortega, K.L. An objective high-resolution hail climatology of the contiguous United States. *Weather. Forecast.* **2012**, *27*, 1235–1248. [CrossRef]
29. Elmore, K.L.; Allen, J.T.; Gerard, A.E. Sub-Severe and Severe Hail. *Weather. Forecast.* **2022**, *37*, 1357–1369. [CrossRef]
30. Schuster, S.S.; Blong, R.J.; Speer, M.S. A hail climatology of the greater Sydney area and New South Wales, Australia. *Int. J. Climatol. J. R. Meteorol. Soc.* **2005**, *25*, 1633–1650. [CrossRef]
31. McMaster, H. Hailstorm risk assessment in rural New South Wales. *Nat. Hazards* **2001**, *24*, 187–196. [CrossRef]
32. Changnon, S.A. Data and approaches for determining hail risk in the contiguous United States. *J. Appl. Meteorol. Climatol.* **1999**, *38*, 1730–1739. [CrossRef]
33. Saltikoff, E.; Tuovinen, J.P.; Kotro, J.; Kuitunen, T.; Hohti, H. A climatological comparison of radar and ground observations of hail in Finland. *J. Appl. Meteorol. Climatol.* **2010**, *49*, 101–114. [CrossRef]
34. Ortega, K.L. Evaluating multi-radar, multi-sensor products for surface hailfall diagnosis. *E-J. Sev. Storms Meteorol.* **2018**, *13*, 1–36. [CrossRef]

35. Dessens, J. Hail in southwestern France. I: Hailfall characteristics and hailstrom environment. *J. Appl. Meteorol. Climatol.* **1986**, *25*, 35–47. [CrossRef]
36. Hohl, R.; Schiesser, H.H.; Aller, D. Hailfall: The relationship between radar-derived hail kinetic energy and hail damage to buildings. *Atmos. Res.* **2002**, *63*, 177–207. [CrossRef]
37. Sioutas, M.; Meaden, T.; Webb, J.D. Hail frequency, distribution and intensity in Northern Greece. *Atmos. Res.* **2009**, *93*, 526–533. [CrossRef]
38. Kaltenboeck, R.; Ryzhkov, A. Comparison of polarimetric signatures of hail at S and C bands for different hail sizes. *Atmos. Res.* **2013**, *123*, 323–336. [CrossRef]
39. Caballol, M.; Méndez-Cartín, A.L.; Serradó, F.; De Caceres, M.; Coll, L.; Oliva, J. Disease in regenerating pine forests linked to temperature and pathogen spillover from the canopy. *J. Ecol.* **2022**, *110*, 2661–2672. [CrossRef]
40. Kopp, J.; Schröer, K.; Schwierz, C.; Hering, A.; Germann, U.; Martius, O. The summer 2021 Switzerland hailstorms: Weather situation, major impacts and unique observational data. *Weather* **2022**. [CrossRef]